



PCCP

**Radicals from tributyl phosphate decomposition: a combined electron paramagnetic resonance spectroscopic and computational chemistry investigation**

Journal:	<i>Physical Chemistry Chemical Physics</i>
Manuscript ID	CP-ART-07-2023-003584.R2
Article Type:	Paper
Date Submitted by the Author:	03-Oct-2023
Complete List of Authors:	Lisouskaya, Aliaksandra; University of Notre Dame, Radiation Laboratory Sosulin, Ilya; University of Notre Dame, Radiation Laboratory Ryan, Delaney; University of Notre Dame, Radiation Laboratory

SCHOLARONE™  
Manuscripts

## ARTICLE

# Radicals from tributyl phosphate decomposition: a combined electron paramagnetic resonance spectroscopic and computational chemistry investigation

Received 00th July 2023,  
Accepted 00th July 2023

DOI: 10.1039/x0xx00000x

Ilya S. Sosulin<sup>a</sup>, Delaney H. Ryan<sup>a,b</sup>, Aliaksandra Lisouskaya<sup>a\*</sup>

The radiation- and chemically-induced radicals from tributyl phosphate (TBP) have been characterized by EPR spectroscopy and theoretical calculations. The yield of X-ray-generated TBP radicals measured by a PBN spin trap is 0.22  $\mu\text{mol/J}$  at room temperature (298 K). The EPR spectra obtained by irradiating TBP with an electron beam at 77 K are in close agreement with literature data for samples irradiated with gamma- and X-rays [<https://doi.org/10.1007/BF02165504>, [https://doi.org/10.1016/1359-0197\(89\)90319-6](https://doi.org/10.1016/1359-0197(89)90319-6)]. Possible conformers of alkyl-type, TBP-derived radicals were analyzed by Density Functional Theory calculations. The main contribution to the experimental spectrum at 77 K is shown to be made by a conformer of the  $\text{CH}_3\cdot\text{CHCH}_2\cdot$  radical, which contains all carbon atoms of the butyl group in the same plane. The EPR spectra of TBP radicals induced by the OH radical in aqueous solution were measured for the first time using a continuous flow system. The formation of the alkyl-type TBP radicals  $\text{CH}_3\cdot\text{CHCH}_2\cdot$ ,  $\cdot\text{CH}_2\text{CH}_2\cdot$ , and  $\cdot\text{CH}_2\text{CHO}$  in the ratio of 5/3/1 was detected; their spectral assignment was based on quantum chemical calculations with simple rotational averaging of HFC constants for the corresponding beta- and alpha-protons.

## Introduction

Tributyl phosphate (TBP) is widely used as a solvent for rare-earth and heavy-element processing.<sup>1</sup> Its performance toward uranium extraction was established during the Manhattan Project in the United States of America.<sup>2</sup> Today, the main role of TBP as an extractant is found in nuclear waste treatment processes.<sup>1</sup> One of the most prevalent, the PUREX process, is connected to the separation of uranium and plutonium from other actinides in acidic nuclear fuel dissolutions.<sup>3</sup> During the separation process, TBP is in contact with radioactive metals and is exposed to radiation, thus the evaluation of its stability is of primary importance.

In the process of nuclear waste separation, radiolysis of a mixture of organic and aqueous phases generates a variety of inorganic and organic radicals. The resulting radicals can enter into secondary reactions with TBP. In the case of aqueous solutions, TBP will react with the primary water radiolysis products, such as solvated electrons, H atoms, and OH radicals.<sup>4</sup> In the presence of nitric acid,  $\text{NO}_3$  radicals could also play a role in the TBP degradation processes. The rate constants for the reactions of TBP with  $e^-$ ,  $\text{H}\cdot$ ,  $\cdot\text{OH}$ , and  $\cdot\text{NO}_3$  in aqueous solutions were measured by pulse radiolysis.<sup>5, 6</sup> Nevertheless, the

detailed mechanism and nature of the radicals derived from TBP under radiolysis in aqueous solutions have not been fully investigated. This is because these TBP organic transients have a short lifetime, as well as an optical absorption in the ultraviolet region, which complicates their identification by pulsed radiolysis techniques.

The radiation stability of TBP was investigated by analyzing the final products.<sup>7</sup> It appeared that molecular hydrogen, di- and mono-butyl phosphates, *n*-butanol, and some other C-2, C-3, and C-4 hydrocarbons were major products of TBP radiation-induced decomposition. An advanced GC-MS-MS technique was used to identify minor decay products including oligomers and fragmentation products in the presence of air and nitric acid.<sup>8</sup> Mostafavi et al. employed picosecond pulse radiolysis to probe the TBP solvated electron ( $e_{\text{TBP}}^-$ ), the TBP triplet excited state, and radical cations.<sup>9</sup> A number of works were also devoted to the analysis of TBP neutral radicals under the action of X-rays and  $\gamma$ -rays.<sup>8, 10, 11</sup> The irradiation at a low temperature (77 K) made it possible to detect alkyl-type radicals with a radiation-chemical yield of 12.9 radicals/100 eV<sup>10</sup> or 6.8 radicals/100 eV.<sup>11</sup> The main contribution to the EPR spectrum, apparently, is made by the  $\text{CH}_3\cdot\text{CHCH}_2\cdot$  type radical with hyperfine coupling (HFC) constants of 2.2, 3.5, and 5.0 mT,<sup>10</sup> but its precise nature is not entirely clear.

The detailed analysis of solid-state EPR spectra is usually quite complicated. As a rule, one should take into account the influence of the *g*-factor and large anisotropic HFC constants, as well as the contribution of the environment of the various paramagnetic species.<sup>12</sup> Conformational variety is present at low temperatures and affects the EPR pattern. Performing quantum chemical calculations is a natural way to solve this

<sup>a</sup> Notre Dame Radiation Laboratory, University of Notre Dame, Notre Dame, IN 46556, USA

<sup>b</sup> Department of Chemical and Biomolecular Engineering, University of Notre Dame, Notre Dame, Indiana 46556, USA

† Footnotes relating to the title and/or authors should appear here.

Electronic Supplementary Information (ESI) available: [details of any supplementary information available should be included here]. See DOI: 10.1039/x0xx00000x

problem. With recent advances in computer development, it is straightforward to estimate the HFC constants for dozens of molecular conformers and find those that match with experimental results. In our study, we investigated the structures of radicals derived from TBP under irradiation at low temperature (77 K) by EPR spectroscopy. The radiation-chemical yield of TBP radicals at room temperature was measured by spin-trapped EPR. We applied the continuous-flow EPR method to analyze the radicals formed in the reaction of TBP with OH radicals at room temperature. The interpretation of the experimental data was based on modern quantum chemical calculations with automatic conformational analysis, which makes it possible to determine both the identities and weights of certain conformers observed in the spectrum.

## Experimental

### Materials

The spin-trap N-tert-butyl- $\alpha$ -phenylnitron (PBN,  $\geq 98\%$ ), Tributyl phosphate (TBP,  $\geq 99\%$ ), Titanium (III) chloride ( $\text{TiCl}_3$ , 10-15%  $\text{TiCl}_3$  basis), Ethylenediaminetetraacetic Acid (EDTA, 99.4%), Iron (II) sulfate heptahydrate ( $\text{FeSO}_4 \cdot 7\text{H}_2\text{O}$ ,  $\geq 99\%$ ), and Sulfuric acid ( $\text{H}_2\text{SO}_4$ , 95.0-98.0%) were purchased from Sigma-Aldrich. Hydrogen peroxide ( $\text{H}_2\text{O}_2$ , 30%) was purchased from EMD Millipore Corporation, (2,2,6,6-Tetramethylpiperidin-1-yl)oxyl (TEMPO, 98%) from Thermo Fisher Scientific, and Potassium thiocyanate (KSCN, 98%) from Alfa Aesar. All solutions were prepared using deionized water from the Serv-A-Pure Co (18 M $\Omega$ -cm resistivity).

### Spin-trapped EPR spectroscopy

Solutions of different PBN concentrations in TBP were used for the spin-trap study. PBN solutions were saturated with Ar to remove atmospheric oxygen, placed in BLAUBRAND<sup>®</sup> disposable micropipettes, and sealed with hot-melt adhesive to prevent leakage. All solutions were prepared fresh before the experiment. Irradiation was carried out with a Thales THX 160 X-ray tube powered by a Spellman DF3 high-voltage power supply (50 kV, 30 mA). The X-ray tube is connected directly to the EPR resonator, which makes it possible to perform *in-situ* irradiation and simultaneously measure the spectrum at room temperature. The dose rate calculated by Fricke dosimetry performed in the same micropipettes ( $G(\text{Fe}^{3+}) = 15.6$  ions/100 eV or 1.6  $\mu\text{mol}/\text{J}$ ) was 211 mGy/s.<sup>13</sup> The dose rate for TBP, which was calculated using the mass absorption coefficients at an effective X-ray energy of ca. 30 keV, was 330 mGy/s.<sup>14</sup> EPR spectra were measured using a Bruker EMXplus spectrometer in X-band (9.87 GHz) with ER4119HS standard resonator. The following parameters were used: microwave power of 0.6325 mW, time constant of 0.01 ms, and modulation amplitude of 0.1 mT. EPR signal intensity was determined as a result of the double integration of the initial EPR spectrum, performed in the Origin Pro software. In the case of fast kinetics measurements, one signal peak at 351.5 mT was recorded and averaged over four scans. The peak intensity was determined as indicated by arrows in Figure 1.

### Low-temperature EPR spectroscopy

150-200  $\mu\text{l}$  of TBP were deoxygenated by the Freeze-Pump-Thaw method in EPR quartz tubes, frozen in liquid nitrogen, and sealed under vacuum. Radiolysis was carried out with 8 MeV electron pulses of about 15 ns duration from an electron linear accelerator in liquid nitrogen at 77 K. The approximate absorbed dose per sample was 200 Gy. The EPR spectra were recorded after irradiation in a liquid nitrogen Dewar flask on an EMXplus Bruker spectrometer equipped with an ER4119HS resonator. Spectra were acquired with 0.6352 mW microwave power, 0.1-0.3 mT modulation amplitude, and a microwave frequency of 9.4 GHz (X-band) at 77 K.

### Continuous flow EPR spectroscopy

Continuous flow EPR experiments were carried out in a  $\text{Ti}^{3+}/\text{EDTA}/\text{H}_2\text{O}_2$ -Fenton system with a Bruker ER 4117 MX-II Dielectric Mixing Resonator installed on a Bruker EMXplus EPR spectrometer in the X-band (9.87 GHz). For each experiment, the solutions were prepared freshly in argon-saturated ultrapure water and stored under an argon atmosphere. For the Fenton-like reaction, 100 mL of each of the two reactant solutions were prepared. Solution 1 consisted of  $\text{TiCl}_3$  (8.8 mM) with EDTA (14 mM) and solution 2 contained TBP with  $\text{H}_2\text{O}_2$  (160 mM). The flow rates were determined by measuring the emptying times of the syringes, and the reaction times were calculated using the geometry of the resonator.<sup>15</sup> To calibrate the mixing ER 4117 MX-II resonator, the reaction between TEMPO (2,2,6,6-tetramethylpiperidinyloxy) and sodium dithionite was used. The following parameters were employed to record the EPR spectra: microwave power of 0.6325 mW, time constant of 0.01 ms, and modulation amplitude of 0.05 mT.

### Quantum chemical calculations

Quantum chemical calculations of radicals derived from TBP in aqueous solutions were performed using the Gaussian 16, Rev. C.01 program package.<sup>16</sup> Optimized geometries of the resulting radical species were obtained using the B3LYP functional with a 6-311+G(d,p) basis set.<sup>17</sup> The solvent effect was modeled by including radicals in a self-consistent reaction field using a polarized cavity model with parameters suitable for water.<sup>18</sup> Isotropic hyperfine coupling constants were obtained by single-point calculations using the B3LYP/gen level, specifically designed for satisfactory recovery of the Fermi contact spin density<sup>19</sup> and the same solvent model.

To efficiently obtain accurate low-temperature rotationally averaged hyperfine couplings, we conducted calculations for various conformers of TBP radicals using a program PRIRODA-04 developed by Laikov.<sup>20</sup> This program includes many unique features, such as modern basis sets for accurate description of molecular parameters,<sup>21, 22</sup> precise parametrizable electronic structure model (QM\_N3),<sup>23</sup> effective algorithms for solving isokinetic equations of motion,<sup>24</sup> and the majority of common theoretical methods based on density functional theory or wavefunction theory (HF, MPX (X=2,3,4), CI, CC, etc.). The QM\_N3 model was used to perform automatic analysis of

conformers. The obtained structures were optimized and HFC constants were computed at the DFT(B3LYP)/L1a\_3 level of theory.<sup>21</sup> A resolution of the identity approach was used to improve performance and reduce the memory overhead for DFT calculations.

## Results and discussion

### Spin-trap study

Irradiation of PBN/TBP solutions leads to the formation of spin adducts. The corresponding EPR spectra are presented in Figure 1. The observed signal is a triplet of doublets with  $a(N) = 1.36$  mT and  $a(H) = 0.18$  mT, which agrees with the literature data on alkyl radicals.<sup>25</sup> We did not observe any contribution from H-trapped adducts. Therefore, under the experimental conditions, PBN traps mainly alkyl radicals formed from TBP.

The efficiency of TBP radiolysis can be evaluated by measuring the radiation-chemical yield ( $G$ -value) of radicals formed. The  $G$ -value derived from the experimental accumulation curves is related to spin-trapped adducts (PBN-TBP\*). In order to estimate the  $G$ -value for TBP-derived radicals, one should consider the competition between the formation and decay of spin-adducts. The simplest kinetic scheme can be specified by the following equations:



where  $\rho$  is TBP density [kg/l],  $G$  is radiation-chemical yield [mol/J],  $I$  is a dose rate [Gy/s],  $k_d$  is the rate constant of the decomposition reaction [1/s],  $k_t$  is the rate constant of the trapping reaction [1/s].

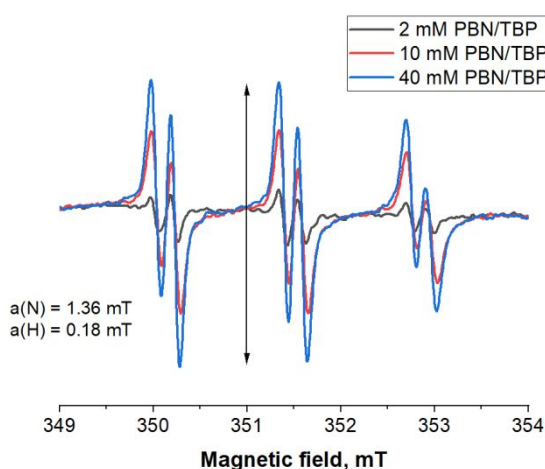


**Figure 1.** Experimental spectrum of X-ray irradiated (absorbed dose ~215 Gy) PBN in TBP solutions saturated with argon. The peak intensity used for kinetic measurements is indicated by the arrow.

Reaction (2) must be bimolecular and include the impurity concentration, which unfortunately cannot be measured. To solve the system of equations, it is necessary to make some simplifications, and the chosen approximation is one of the most natural in this case.

Assuming the steady-state approximation for  $\text{TBP}^*$ , we can express the formation rate of the spin adduct  $\text{A}^*$ :

$$\frac{d\text{A}^*}{dt} = \frac{k_d \rho G I}{k_d + k_t [\text{PBN}]} [\text{PBN}] \quad (4)$$

This functional form of the decay kinetics assumes the reaction follows a pseudo-first order. The rate constant is achieved by processing the spin adduct formation curve (Figure 2).

$$\text{A}^* = [\text{PBN}] (1 - e^{-k_{\text{exp}} t}) \quad (5)$$

Measurement of three experimental rate constants ( $k_{\text{exp}1}$ ,  $k_{\text{exp}2}$ ,  $k_{\text{exp}3}$ ) with three distinct PBN concentrations ( $[\text{PBN}]_1$ ,  $[\text{PBN}]_2$ ,  $[\text{PBN}]_3$ ) gives a system of three equations with three unknown variables:  $k_d$ ,  $k_t$ , and  $G$ . One can then introduce  $b$  as (6).

$$b = \frac{k_{\text{exp}1} - k_{\text{exp}2}}{k_{\text{exp}2} [\text{PBN}]_2 - k_{\text{exp}1} [\text{PBN}]_1} \quad (6)$$

And then express the  $G$ -value as (7).

$$G = \frac{k_{\text{exp}3} + k_{\text{exp}3} [\text{PBN}]_3 b}{b I} \quad (7)$$

Figure 2 shows spin adduct accumulation curves for 2 mM, 10 mM, and 40 mM PBN in TBP. The corresponding  $G$ -value for the formation of TBP-derived radicals is 0.22  $\mu\text{mol/J}$  (2.1 radicals/100 eV) or at room temperature (298 K). The low-temperature experiments reported by Kuruc or Haase gave higher values (12.9 or 5.5 radicals/100 eV),<sup>10, 11</sup> which may be due to hindered diffusion and therefore decreased the chance of radical recombination at low temperatures.

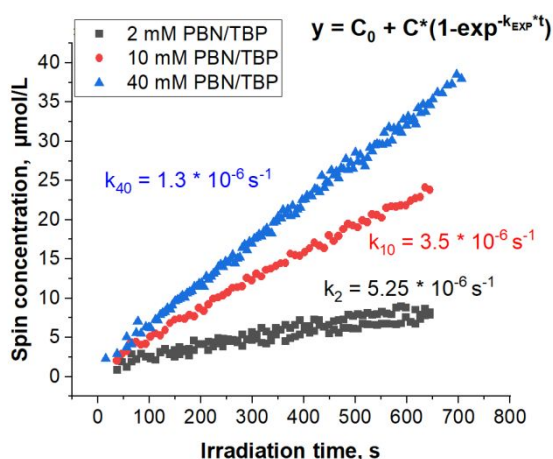


**Figure 2.** Formation curves of PBN-TBP adducts for 2 mM, 10 mM, and 40 mM PBN in TBP. Reaction rate constants from fitting shown in the figure with color code.

Previously, it was reported that the  $G$ -value of TBP decay upon  $\gamma$ -irradiation at room temperature is 5.5 molec/100 eV.<sup>7</sup> The  $G$ -values of alkane-derived radicals from  $C_5 - C_9$  hydrocarbons at room temperature, measured using the same approach, are in the range of 1.6-1.7 radical/100 eV,<sup>26</sup> which agrees with our results.

### Low-temperature study

The EPR spectrum of irradiated TBP at 77 K is presented in Figure 3. The observed spectrum demonstrates six lines and coincides with previous findings.<sup>10, 11, 27</sup> Irradiation of solid organic compounds at 77 K usually leads to the formation of H-abstraction radicals without breaking the C-C, C-O, or C-N bonds. This is determined by the nature of parental ions or excited states and by the cage effect, which can be crucial in condensed phases. Regarding the structure of TBP, one could expect the formation of four radicals with radical centers on carbon atoms in different positions of the chain (R1-R4), presented in Figure 4. To determine the structure of the radicals and their conformers obtained in the actual experiment, an automatic conformational analysis of the radicals R1 – R4 was carried out. Based on the initial structure of the TBP radical, we performed an isokinetic thermostat simulation (the potential energy surface (PES) was calculated at the QM\_N3 level of theory) according to the original article<sup>24</sup> and collected every 128<sup>th</sup> point geometry from the trajectory. The corresponding structures (the total number was about 20000) were used as input to minimize energy at the same level of theory. The obtained optimized structures (PES minima) were sieved to remove duplicates and then sorted by their energies; the total number of unique conformers was reduced to ~1000. We considered 50 of the lowest energy structures, reoptimized, and computed EPR parameters at the DFT(B3LYP)/L1a\_3 level of theory. The energy difference between the highest and the lowest energy conformers was about 5 kcal/mol.

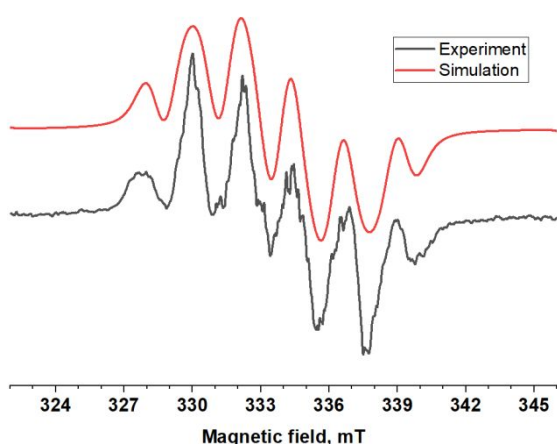


**Figure 3.** Experimental and simulated EPR spectra of electron-irradiated TBP at 77 K (the absorbed dose is approximately 200 Gy). Simulated EPR spectra of the total contribution of radicals are shown in red. Simulated HFCs are presented in Table 1 (EXP).

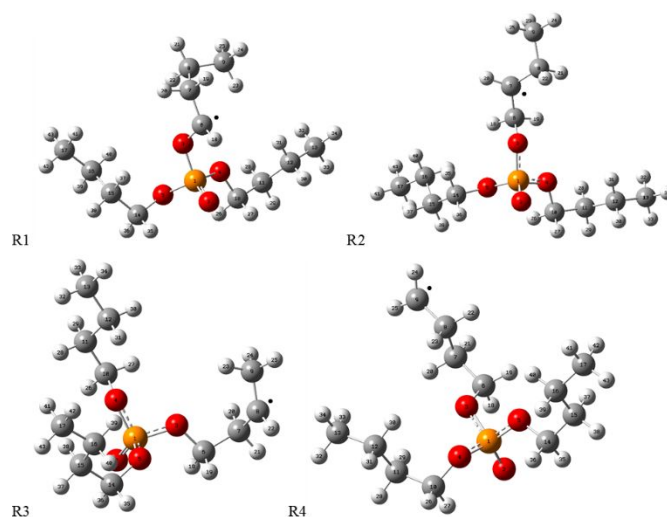


**Figure 4.** Structures of TBP-derived radicals R1 – R4.

Radicals R1 and R4 are possible candidates formed from TBP at 77K.

The absolute values of the calculated HFC constants seem to be overestimated, but it may be useful to consider the relative values. In the case of the R1 radical, the signal should be split by one  $\alpha$ -proton, two  $\beta$ -protons, and the P atom. Theoretical analysis of the R1 radical ( $-\text{CH}_2^*\text{CHO}-$ ) predicts four conformers with different HFC patterns (Table 1). All conformers have relatively small HFC constant on the P atom, which is about the linewidth and should lead to line broadening. The total width of the experimental EPR signal is significantly broader than that calculated for radical R1 conformers. For radical R4 ( $^*\text{CH}_2\text{CH}_2-$ ), HFC splitting from two  $\alpha$ -H and two  $\beta$ -H protons is expected. According to the computational results presented in Table 1, three conformers for radical R4 could be distinguished by the HFC constant for one  $\beta$ -proton. However, the experimental spectrum reveals the contribution of five protons, which is inconsistent with these results. Therefore, the contribution of R1 and R4 radicals can be excluded.

The radical R2 ( $-\text{CH}_2^*\text{CHCH}_2-$ ) has five protons, which corresponds to the pattern of the experimental spectrum. Moreover, some previous papers<sup>10, 11</sup> indicate up to 20% of the contribution of this radical to the entire spectrum. Conformational analysis reveals two conformers for radical R2, as shown in Table 1. However, both R2 conformers are not consistent with the observed spectrum.

Radical 3 ( $\text{CH}_3^*\text{CHCH}_2-$ ) has five beta protons - three on the methyl group and two on the methylene group - as well as one alpha proton. Considering radical R3, one would expect two conformers: all carbon atoms of the butyl group are located virtually in one plane (R3-A) or in twisted configurations (R3-B). Visual representations of these cases are depicted in Figure 5.

**Table 1** Experimental and calculated HFC constants for conformers of radicals R1, R2, R3, and R4 at the DFT(B3LYP)/L1a\_3 level of theory. HFC constants and linewidths are in mT.

	a( $\alpha$ -H)	a <sub>1</sub> ( $\beta$ -H)	a <sub>2</sub> ( $\beta$ -H)	a <sub>3</sub> ( $\beta$ -H)	a <sub>4</sub> ( $\beta$ -H)	a <sub>5</sub> ( $\beta$ -H)	a(P)
R1							
R1-A	-1.54	4.05	0.08	-	-	-	0.27
R1-B	-2.34	1.10	1.08	-	-	-	0.30
R1-C	-1.58	1.35	0.74	-	-	-	0.24
R1-D	-2.17	1.95	0.36	-	-	-	0.62
R2							
R2-A	-2.13	1.75	0.04	0.97	4.82	-	-
R2-B	-2.12	1.37	0.13	1.89	4.89	-	-
R4							
R4-A	-2.26; -2.26	5.12	2.46	-	-	-	-
R4-B	-2.28; -2.31	4.75	3.21	-	-	-	-
R4-C	-2.20; -2.24	5.46	1.22	-	-	-	-
R3							
R3-A	-2.33	4.26	2.28	0.29	2.80	4.68	-
R3-B	-2.26	1.97	0.49	0.96	1.71	5.45	-
EXP							
EXP	2.20	2.57	1.43	0.26	2.01	2.70	-

Calculated HFC constants for R3-A and R3-B conformers are presented in Table 1. Performed calculations indicate R3-A conformer has two  $\beta$ -protons with relatively high values, about 4 mT, and one with low, 0.29 mT. The R3-B conformer demonstrates only one  $\beta$ -proton with a large hyperfine constant of 5.45 mT and two small splittings from  $\beta$ -protons.

The experimental EPR spectrum can be described by the splitting from an alkyl radical with one proton  $\alpha$ -H (2.21 mT) and five beta protons  $\beta$ -H (from 0.3 to 2.7 mT), linewidth is 0.57 mT,  $g$ -factor is 2.0019. The HFCs derived from the fitting are summarized in Table 1 (EXP). Comparing the calculated EPR patterns for various conformers, we can conclude that the R3-A radical conformer is formed at low temperatures during the radiolysis of TBP.

### Continuous flow study

The continuous flow EPR system was used to obtain both structural and kinetic information on the radicals formed in the reaction of the OH radical with TBP. OH radicals were generated using a  $\text{Ti}^{3+}/\text{H}_2\text{O}_2$ -Fenton system (8) at room temperature as previously described.<sup>28</sup>

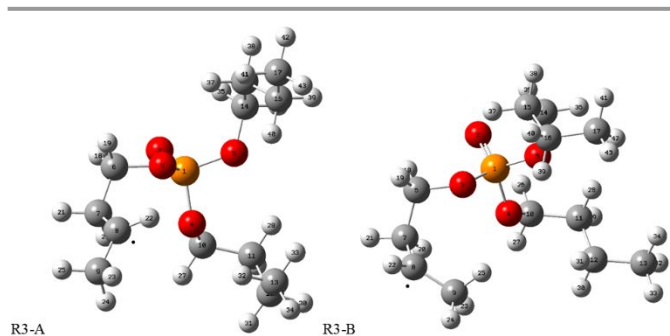


**Figure 5.** Examples of radical R3 conformers with different butyl group configurations (R3-A and R3-B, see text for details).



The solubility of TBP in aqueous solutions is low (about 1.5 mM (0.4 g/L) at room temperature). Despite this, we managed to register an EPR signal of the radicals formed in the reaction with the OH radical. Figure 6 shows EPR spectra of radicals formed in the reaction TBP with  $\cdot\text{OH}$  at neutral pH taken in a fast flow regime.

The obtained EPR signal is weak due to the low concentration of TBP. However, it was possible to measure the kinetics of the central signal depending on the reaction time (see Figure 7). It was found that these radicals are generated very fast and then decay rapidly.

The rates of the reaction of the OH radical with TBP in aqueous solutions were measured earlier by the method of pulsed radiolysis using competition kinetics.<sup>5, 29</sup> The reaction rate constant in neutral media was about  $5 \times 10^9 \text{ M}^{-1}\text{s}^{-1}$ , and in acidic media the value was two times higher, reaching  $1 \times 10^{10} \text{ M}^{-1}\text{s}^{-1}$ .<sup>5, 29</sup> We carried out experiments at different pH values in aqueous solutions.

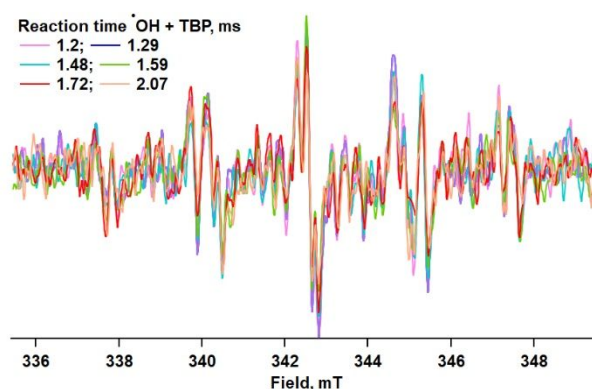


**Figure 6.** EPR spectra of radicals generated in the reaction of the  $\text{Ti}^{3+}/\text{H}_2\text{O}_2$ -Fenton reagent with TBP in aqueous solutions at room temperature.

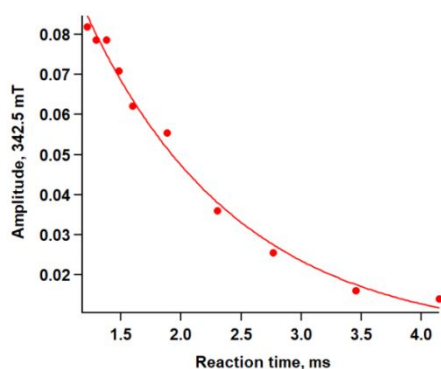


**Figure 7.** Reaction kinetics for TBP with OH radical at room temperature. The EPR signal intensity for radicals generated in the reaction of  $\text{Ti}^{3+}/\text{H}_2\text{O}_2$ -Fenton with TBP (the signal line amplitude) vs. reaction time fitted to the exponential decay.

We found that in acidic solutions, as well as in alkaline solutions, the EPR signal is lost, which can be explained by the solubility of the TBP compound. The half-life of the decay curve is about 2 ms and follows a trend of exponential decay. Under our experimental conditions, the decay kinetics of TBP can be described by self-recombination and disproportionation reactions. The oxidation of TBP radicals by  $\text{Ti}^{4+}$  or  $\text{H}_2\text{O}_2$  can be neglected because their rate constants are much smaller than the rate constant of self-recombination.<sup>30</sup>

The EPR spectrum derived from the reaction of TBP with OH radical shows a large number of peaks originating from individual radicals (Figure 6). After careful spectral analysis, we were able to find that at least three alkyl carbon-centered radicals were formed during the reaction. As described in the literature,<sup>31, 32</sup> a typical alkyl radical  $-\text{CH}_2\cdot\text{CHCH}_2-$  should give major HFCs from beta protons of about 2 – 3 mT and about 2.1 – 2.3 mT from the alpha proton at room temperature.

The simulated spectra of the TBP radicals are superimposed on the experimental spectra in Figure 8.

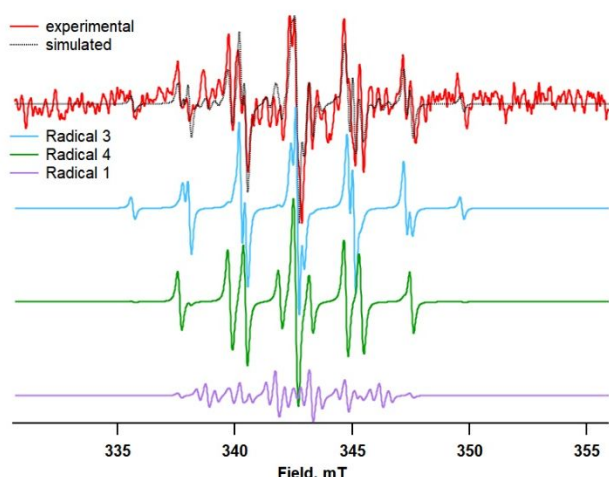


**Figure 8.** Experimental and simulated EPR spectra of radicals generated in the reaction of the  $\text{Ti}^{3+}/\text{H}_2\text{O}_2$ -Fenton reagent with TBP in aqueous solutions at room temperature. Simulated EPR spectra of the total contribution of radicals are shown in black. Simulated parameters: **R3**, 52%  $g = 2.0022$ ; **R4**, 37%  $g = 2.0027$ ; **R1**, 10%  $g = 2.00307$ . Simulated HFCs are presented in Table 1 (EXP).

Based on the calculated data, we predict the formation of the R3 radical, 53%, while the second component corresponding to the R4 radical, 37%. The contribution of the radical R1 was 10%. We did not find a contribution of the R2 radical, which should have six lines from the splitting of five protons.

To confirm the structure of the radicals, we carried out additional calculations. The standard approach involved the DFT calculations in polarized cavity model (iefpcm) of structures of H-loss radicals from TBP in reaction with OH radical in aqueous solutions as explained in the Methods section. The calculated EPR parameters for the main conformers of potential radicals are given in Table 2. The optimized geometries of radicals are presented in Table S2. It is assumed that the temperature should influence the hyperfine splitting constants, largely due to the internal rotation of the torsion barriers. Based on the experimental data presented in the work by Fessenden and Schuler,<sup>31</sup> we expected that the change in the temperature of the proton constants of alkyl radicals would be less noticeable. Since the TBP-derived radicals are not conformationally rigid in an aqueous medium at room temperature, as in the case of 77 K, the rotationally-averaged HFC constants for the beta-protons can be calculated. We scanned the PES of radicals at the DFT(B3LYP)/L1a\_3 level of theory by changing the dihedral angle  $\alpha\text{H-C-C-}\beta\text{H}$  from 2 to 355 degrees and extracting HFC constants for each of the 49 points. We used dimethyl butylphosphate radicals, which are isostructural with the R1-R4 radicals of TBP, to simplify the computational problem. This assumption is justified when other butyl groups are not affected by radical spin density distribution (the corresponding values on the  $\text{CH}_2$  fragments adjacent to the oxygen atoms are negligible). The observed HFC values were determined by the Boltzmann distribution at 298 K<sup>33</sup>:

$$a = \frac{\sum_i e^{-\frac{E(Q_i)}{kT}} a(Q_i)}{\sum_i e^{-\frac{E(Q_i)}{kT}}} \quad (8)$$

where the integration along the pseudorotation coordinate  $Q$  is replaced with the summation over the  $Q_i$  set of points for which the calculated values of energy  $E(Q_i)$  and the HFC constants  $a(Q_i)$  are available. The resulting average HFC constants calculated this way are presented in Table 2. The angular dependences of HFC constants on beta protons and alpha proton for radical R3 are shown in Figure 9; data for other radicals are shown in Figures S1-S3. As follows from Table 2, close agreement between experimental and theoretical data confirms the formation of R3, R4, and R1 radicals in the continuous flow system experiments.

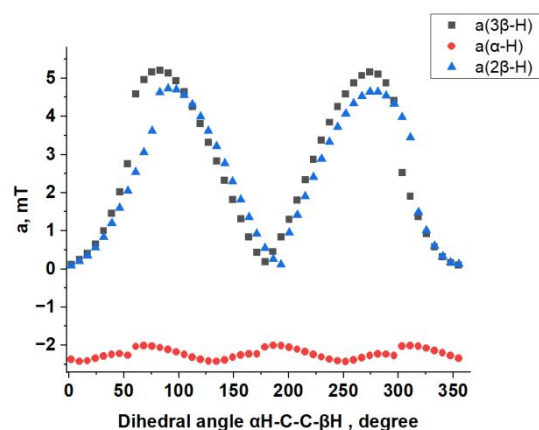


**Figure 9.** The HFC constants for alpha and beta-protons of radical R3, calculated at the DFT(B3LYP)/L1a\_3 level of theory as a function of dihedral angle  $\alpha\text{H-C-C-}\beta\text{H}$ .

**Table 2.** Experimental fitting parameters for the EPR spectrum of radicals generated in the reaction of the  $\text{Ti}^{3+}/\text{H}_2\text{O}_2$ -Fenton reagent with TBP in aqueous solutions at room temperature, calculated rotationally averaged HFC constants for radicals R1 – R4 at the DFT(B3LYP)/L1a\_3 level of theory and averaged HFC constants for radicals R1 – R4 at the B3LYP/gen (iefpcm). HFC constants and linewidths are given in mT.

	$a(\alpha\text{-H})$	$a_1(\beta\text{-H})$	$a_2(\beta\text{-H or } \gamma\text{-H})$
R1			
EXP	1.46 (1H)	2.98 (2H)	0.38 (2H)
B3LYP/gen	1.47 (1H)	3.15 (2H)	0.06 (2H)
B3LYP/L1a_3 rot. averaged	1.89 (1H)	3.22 (2H)	-
R2			
EXP	-	-	-
B3LYP/gen	1.94 (1H)	2.38 (4H)	3.28 (2H)
B3LYP/L1a_3 rot. averaged	-2.18 (1H)	1.73 (2H)	2.59 (2H)
R3			
EXP	2.2 (1H)	2.4 (5H)	
B3LYP/gen	2.05 (1H)	2.95 (2H)	2.65 (3H)
B3LYP/L1a_3 rot. averaged	-2.24 (1H)	2.58 (2H)	2.63 (3H)
R4			
EXP	2.16 (2H)	2.8 (2H)	
B3LYP/gen	2.23 (2H)	3.40 (2H)	
B3LYP/L1a_3 rot. averaged	-2.28 (2H)	2.72 (2H)	

## Conclusions

In this work, a systematic investigation of radicals derived from TBP was performed. The efficiency of radiation-induced radical formation at room temperature was first evaluated by the PBN spin-trapping approach. The corresponding  $G$ -value for  $\text{TBP}^{\bullet}$  is  $0.22 \mu\text{mol/J}$ , which is in agreement with literature data for alkanes under the same conditions.

The recorded EPR spectrum of neat TBP irradiated at 77 K displays signals from alkyl radicals. Careful analysis of the spectrum indicates the main contribution of the carbon-centered radical with four beta-protons and one alpha-proton, formed upon H-abstraction from one of the two middle methylene groups of TBP. An automatic conformational analysis on four TBP-derived radicals was performed to investigate the

possible radical conformations. From these calculations, four conformers were found for the radical R1, two for the radicals R2 and R3, and three for the radical R4 (Table 1). The calculated HFC constants of the R3-A conformer, in which all four carbon atoms of the butyl group lie in the same plane, are in good agreement with the observed spectrum. At the same time, other conformers of R2, R3, and R4 could be excluded based on the computed EPR parameters. Thus, one can conclude that the EPR spectrum of irradiated TBP at 77 K corresponds to the conformer A of the R3 TBP radical.

A continuous flow EPR method was used to study the reactions of TBP with the OH radical in aqueous solutions at room temperature. The half-life of the resulting TBP radicals is about 2 ms and follows an exponential decay. After careful spectral analysis, we were able to find that at least three carbon-centered alkyl radicals are formed during the reaction of TBP with  $\bullet\text{OH}$ . Based on the calculated data, we predicted the formation of the R3 and R4 radicals, with a small contribution from the R1 radical. Radical 3 makes the largest contribution to the structure of the spectrum, as seen in Figure 8, which is consistent with the data obtained at low temperatures. The obtained data point to the main contribution of the similar carbon-centered radical formed upon irradiation of pure TBP and TBP dissolved in water. This suggests an H atom abstraction mechanism for the potential long-term effects of irradiation on the TBP particles present during separation.

The results obtained in this work are of great importance for the radiation chemistry of TBP used for nuclear waste separation. These data make it possible to estimate the radiation resistance and determine the structure of radical conformers induced by irradiation with X-rays or electron beams, and chemically generated.

## Author Contributions

Ilya S. Sosulin: Planned the experiments, collected the data, performed the analysis, performed theoretical calculations, and wrote the original draft of the manuscript.

Delaney H. Ryan: Collected the data, performed the analysis, and contributed to the writing of the manuscript.

Aliaksandra Lisouskaya: Directed the project, performed the analysis, performed theoretical calculations, and reviewed and edited the manuscript.

All authors discussed the results and contributed to the final manuscript.

## Conflicts of interest

There are no conflicts to declare.

## Acknowledgements

This work is supported by the U.S. Department of Energy, Office of Science, Office of Basic Energy Sciences under award number DE-FC02-04ER15533. Quantum chemical calculations were performed on machines in the Center for Research Computing

at the University of Notre Dame. This is document number NDRL-5407 from the Notre Dame Radiation Laboratory. The authors thank Prof. I. Carmichael, K.R. Briling, and Dr. D.N. Laikov for valuable discussions and suggestions on the theoretical analysis.

## Notes and references

**Supporting Information.** Optimized molecular geometries of TBP conformers, HFC constants of radicals R2, R2, and R4 depending on the dihedral angle  $\alpha$ H-C-C- $\beta$ H.

## References

1. W. W. Schulz, K. P. Bender, L. L. Burger and J. D. Navratil, *Science and technology of tributyl phosphate*, United States, 1990.
2. A. Naylor and H. Eccles, USSR, 1988.
3. H. A. C. McKay, *The PUREX process*, CRC Press, Inc, United States, 1990.
4. G. V. Buxton, C. L. Greenstock, W. P. Helman and A. B. Ross, *Journal of Physical and Chemical Reference Data*, 1988, **17**, 513-886.
5. B. J. Mincher, S. P. Mezyk and L. R. Martin, *The Journal of Physical Chemistry A*, 2008, **112**, 6275-6280.
6. J. O. Dziegielewski and K. Filipek, *Journal of Radioanalytical and Nuclear Chemistry*, 1988, **128**, 109-116.
7. J. G. Burr, *Radiation Research*, 1958, **8**, 214-221.
8. D. Lesage, H. Virelizier, C. K. Jankowski and J. C. Tabet, *Spectroscopy*, 1997, **13**, 275-290.
9. F. Wang, G. P. Horne, P. Pernot, P. Archirel and M. Mostafavi, *The Journal of Physical Chemistry B*, 2018, **122**, 7134-7142.
10. J. Kuruc, V. E. Zubarev, L. T. Bugaenko and F. Macásek, *Journal of Radioanalytical and Nuclear Chemistry*, 1988, **127**, 37-49.
11. K. D. Haase, D. Schulte-Frohlinde, P. Kouřim and K. Vacek, *International Journal for Radiation Physics and Chemistry*, 1973, **5**, 351-360.
12. J. A. Weil and J. R. Bolton, *Electron Paramagnetic Resonance: Elementary Theory and Practical Applications*, Wiley, 2006.
13. F. H. Attix, W. C. Roesch and E. Tochilin, *Radiation dosimetry*, Academic Press, New York [etc.], 2nd edn., 1966.
14. J. H. Hubbell and S. M. Seltzer, *Tables of x-ray mass attenuation coefficients and mass energy-absorption coefficients 1 keV to 20 MeV for elements Z = 1 to 92 and 48 additional substances of dosimetric interest*, United States, 1995.
15. E. Schubert, T. Hett, O. Schiemann and Y. Nejatjahromy, *J. Magn. Reson.*, 2016, **265**, 10-15.
16. M. J. Frisch, G. W. Trucks, H. E. Schlegel, G. E. Scuseria, M. A. Robb, J. R. Cheeseman, G. Scalmani, V. Barone, G. A. Petersson, F. O, J. B. Foresman and J. D. Fox, *Journal*, 2016.
17. T. H. Dunning, *The Journal of Chemical Physics*, 1989, **90**, 1007-1023.
18. G. Scalmani and M. J. Frisch, *The Journal of chemical physics*, 2010, **132**, 114110.
19. R. Stenutz, I. Carmichael, G. Widmalm and A. S. Serianni, *J. Org. Chem.*, 2002, **67**, 949-958.
20. D. N. Laikov and Y. A. Ustynyuk, *Russian Chemical Bulletin*, 2005, **54**, 820-826.
21. D. N. Laikov, *Theoretical Chemistry Accounts*, 2019, **138**, 40.
22. D. N. Laikov, *Chemical Physics Letters*, 2005, **416**, 116-120.
23. D. N. Laikov, *The Journal of Chemical Physics*, 2011, **135**.
24. D. N. Laikov, *Theoretical Chemistry Accounts*, 2018, **137**, 140.
25. G. R. Buettner, *Free Radical Biology and Medicine*, 1987, **3**, 259-303.
26. V. N. Belevskii and S. I. Belopushkin, *High Energy Chemistry*, 2005, **39**, 1-9.
27. S. Huai-Yu, W. Zhi-Zhong, C. Yao-Huan, H. Yong-Hai, W. Qi-Zhong, C. Jin-Tai and L. Ren-Zhong, *International Journal of Radiation Physics and Chemistry*, 1989, **33**, 585-597.
28. A. Lisovskaya, O. Shadyro, O. Schiemann and I. Carmichael, *PCCP*, 2021, **23**, 1639-1648.
29. P. G. Clay and M. Witort, *Radiochemical and Radioanalytical Letters*, 1974, **19**, 101-107.
30. S. Croft, B. C. Gilbert, J. R. Smith and A. C. Whitwood, *Free Radic Res Commun*, 1992, **17**, 21-39.
31. R. W. Fessenden and R. H. Schuler, *J. Chem. Phys.*, 1963, **39**, 2147-2195.
32. H. Fischer, *J. Phys. Chem.*, 1969, **73**, 3834-3838.
33. S. V. Blinkova, L. N. Shchegoleva, I. V. Beregovaya, M. M. Vyushkova, V. A. Bagryansky and Y. N. Molin, *Applied Magnetic Resonance*, 2011, **41**, 229-238.